

Calculating the Dynamic Behaviour of Rotating Beams Affected by Transverse Cracks

N. Bachschmid¹ and E. Tanzi²

¹ Politecnico di Milano, Via La Masa, 34 I 20158 Milano nicolo.bachschmid@polimi.it

² ezio.tanzi@mecc.polimi.it

***ABSTRACT.** This paper presents an overview of the different models which have been used for analysing and simulating the static and dynamic behaviour of rotating shafts presenting a transverse crack. The simplified model which has been developed by the authors is described and compared to other models with regards to simplicity and accuracy.*

INTRODUCTION

The modelling of cracked rotating shafts has been the aim of many researchers in the last 30 years. More than 150 papers on this topic have been recorded. State of art reviews have been published in [1, 2, 3]. But there are still some points which are not completely covered by the investigations, and some aspects of the modelling process which are not well understood. The peculiarity of the behavior of cracked rotating shafts is that the opening and closing of the crack during one rotation occurs gradually, whilst that one of a vibrating cracked beam occurs suddenly, generating a non-linear behavior.

The gradually opening and closing mechanism of transverse cracks in rotating shafts is the well-known breathing mechanism. The presence of the crack in a beam affects its stiffness: an open deep crack lowers the stiffness of the complete shaft by a generally small amount. A closed crack leaves its stiffness apparently unaffected. The gradually changing of the shaft stiffness due to the breathing mechanism is the main cause of the vibrations experienced by cracked shafts. In order to simulate the dynamic behavior of cracked rotors different models are needed: a model for reproducing the breathing mechanism, a model for calculating the reduction in stiffness of the beam, and a model for simulating the dynamic behavior of rotating cracked shafts.

MODEL OF THE BREATHING MECHANISM

The breathing mechanism is a result of the stress and strain distribution around the cracked area, which is due to static loads, like the weight, the bearing reaction forces, etc., and dynamic loads, like the unbalance and the vibration induced inertia force distribution. Accurate modelling of the breathing mechanism has been generally

disregarded. When the static loads overcome the dynamic ones, the breathing is governed by the rotation angle with respect to the stationary load direction, and the crack opens and closes again completely once each revolution. The transition from closed crack (full) stiffness to the open crack (weak) stiffness has been generally considered abrupt or represented by a given cosine function.

3D non linear finite element calculations allow to predict accurately the breathing mechanism, when the loads are known, but are extremely cumbersome, costly and time consuming (due to the need of a refined mesh in the crack region, and to the non-linear contact conditions).

A simplified model, which assumes linear stress and strain distributions, for calculating the breathing behavior, has been developed by the authors and proved to be very accurate. Breathing behavior determining is a non-linear iterative procedure. The breathing mechanism is affected also by transient thermal stresses which can arise in rotating shafts during a change in operating conditions, and by pre-stresses which can develop during the crack propagation. These pre-stresses can further open the crack or can tend to hold the crack more closed, influencing the breathing behavior. Also these aspects have been completely disregarded in previous investigations.

Simplified Model for Breathing Mechanism Calculation

In the following, the different steps for modeling the breathing behavior, including thermal effects, are illustrated:

- a) In correspondence of the cracked section, the cross sectional area A is divided into small area elements $dA = dx dy$ according to a rotating reference system (fixed on the rotor) $x'y'$ (Fig. 1);
- b) The bending moment M due to the weight and the bearing alignment conditions of the rotor is calculated in correspondence of the cracked section.
- c) One revolution (360°) of the shaft is divided in 128 parts: in each position following calculations are performed (from d) to e)):

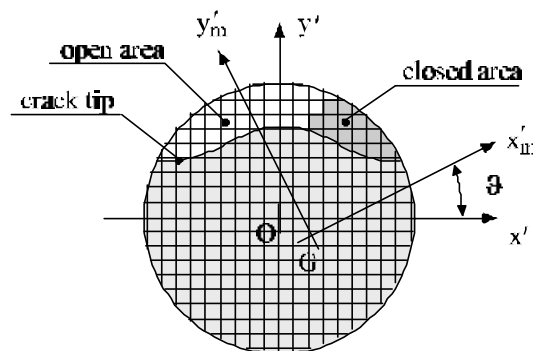


Figure 1. Cracked cross section.

- d) An iterative procedure is started in order to define the open and closed sections of the cracked area, the position of the center of gravity G of the closed surface, the position of the main axes of inertia (angle ϑ) with origin in G , the second area

moments with respect to the main axes and the moments M_{xp} , M_{yp} due to the thermal stress distribution;

- d₁) Initially the main axes (x'_m , y'_m) are considered to be coincident with the rotating crack axes (x' , y'); the stresses due to bending moment are calculated (with the assumed x'_m , y'_m main axes), and the thermal stresses are then added in each point;
- d₂) Now the stress distribution is known over the cross section and the sign of the stress can be checked in each point of the cracked area: '+' means tension and therefore we have no contact forces in this point (the crack area element is "open"), '-' means compression and therefore we have contact forces (the crack area element is "closed"). The open and closed area sections have been determined.
- d₃) The surface gravity center of the total area (formed by the uncracked area plus the closed cracked area) can be calculated.
- d₄) The second moments of area can now be calculated with respect to reference system (x' , y') with origin in G and the angular position ϑ of the main axes of inertia (x'_m , y'_m) can be found;
- d₅) Now the procedure from (d₁) to (d₄) is repeated until ϑ converges to a stable value;
- e) At this point the position of the main axis and the second area moments and M_{xm} , M_{ym} are known. The second area moment J_x , J_y and J_{xy} with respect to the fixed reference frame (x , y) and the components of the moments due to the thermal stress distribution (M_x , M_y) with respect to the same reference frame are calculated. This will be repeated for each angular position of the shaft.
- f) A Fourier analysis over 128 values of J_x , J_y and J_{xy} and M_x and M_y is carried out, and the mean values J_{xm} , J_{ym} , J_{xym} and their first five harmonic components are extracted.

Breathing Mechanism Validation by means of 3D Non Linear Model

The breathing mechanism calculated with the described simplified approach, has been validated with numerical results obtained with a 3D model of a cracked cylindrical beam, clamped at one end and loaded mechanically at the other end with a rotating load. Also temperature gradients have been imposed to the outer surface of the cylindrical specimen.

Generally an excellent agreement has been found between the simplified linear model and the 3D non-linear model. Fig. 2 and Fig. 3 show the comparison of 3D results in the position where the rotor (or the load) is rotated by 75°, for the 25 % and the 50% depth crack, with the simplified model results: a very good agreement has been found as also in all the other positions. The dark areas are closed, the white areas of the crack are open.

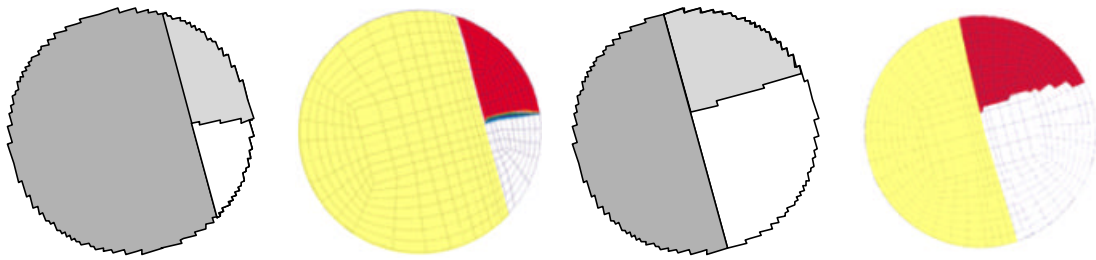


Figure 2. Comparison between the results of the simplified model (left) and the 3D f.e. model (right) for two diff. crack depths (25% and 50%), rotation angle of 75° .

When a thermal transient is superposed to the mechanical loading, then the agreement is found in general to be good. This is shown in Fig. 3 where the angular positions of 120° and 180° are represented in case of negative thermal transient, applied to a 50% deep crack.

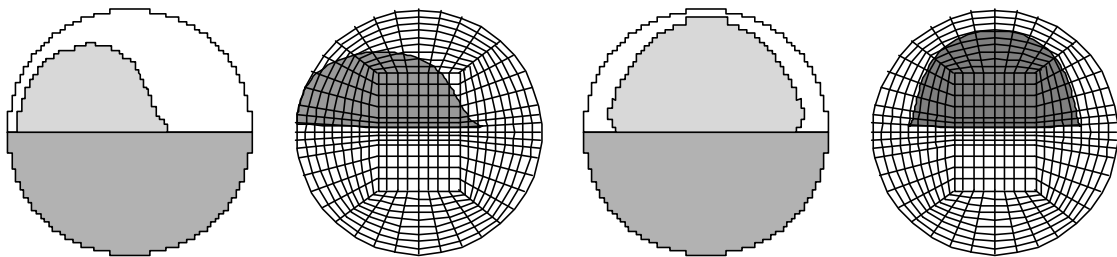


Figure 3. Thermal and mechanical load – Negative gradient – Angular positions 120° and 180° , results of simplified model (left) and 3D model (right).

MODEL OF THE “LOCAL STIFFNESS” OF THE CRACKED SECTION

Different models have been proposed by different researchers, and the results are compared.

The SERR Model

Since the *strain energy release rate* (SERR) approach combined with the stress intensity factors (SIF) had been used by almost all authors (as it is shown in [1, 2, 3]) for the calculations of the cracked beam bending behaviour, several calculations according to this approach and for different crack depths have been made. This approach allows to calculate the additional flexibility introduced by the crack, when the crack is open. Nothing can be said when the crack is half open and half closed, due to the breathing mechanism. Very deep cracks (more than 50% deep) as well as multiple cracks on the same cross section cannot be dealt with this approach. In this case, for making a comparison, the “breathing” mechanism was assumed known (from FEM or from simplified model) and the SERR approach was applied to the cracked cross section, with its open and closed portions, in order to calculate the beam bending

stiffness. The extension of this approach to the breathing crack is affected by some errors due to the fact that the crack tip is supposed to be formed by the boundary between the cracked areas and the uncracked areas for the regions in which the breathing crack is “open”, which is correct, and by the boundary between the “closed” cracked areas and the “open” cracked areas, which is not correct because on this boundary no stress intensity factors will appear.

The approach assumes planar stress and strain distributions (as they are in rectangular cross sections), and no interaction between parallel “rectangular slices” in which the circular cross section has been divided. This is not realistic, as it is shown in Fig. 4, where stress and strain along the crack tip are shown, as a result of 3D calculation.

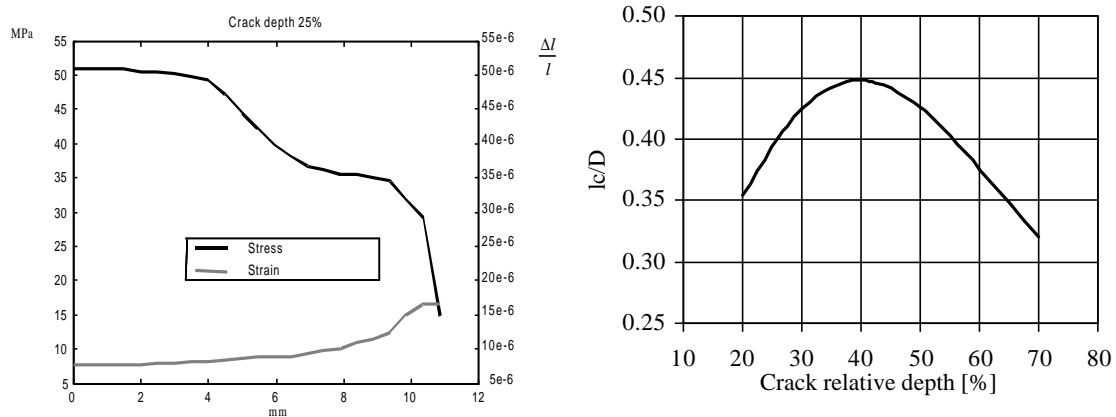


Figure 4. (left) Distribution of axial strains and stresses along the tip of a 25% deep crack, from middle to the end of the crack. (right) Ratio of equivalent length l_c of the cracked beam to its diameter D , as a function of its relative depth.

The cracked cross section is not any more planar, but is distorted. This is not taken into account by the fracture mechanics approach. The fracture mechanics approach further does not consider any friction on the cracked area, and this also seems to be unrealistic. If torsion is present the contribution of friction forces on the cracked area can be taken into account only by the non-linear 3D calculation, and in an approximate way by the simplified model. Nevertheless the results obtained with this approach are very accurate as regards the additional flexibility introduced by the crack, for a completely open crack, as well as for providing stress intensity factor at the crack tip, which are extremely important for evaluating the propagation mechanism. The results obtained with this model will be called SERR results. The additional flexibility can be easily transformed in local crack stiffness.

The Flex Model

Once the breathing mechanism and the second moments of area have been defined for the different angular positions, as previously described, the stiffness matrix of the cracked element of suitable length can be calculated, assuming a Timoshenko beam.

The angular position stiffness matrix $K_c(\Omega t)$ has one constant term (the mean stiffness) and up to five harmonic components which are considered in following calculations. This model is called Flex Model.

The stiffness matrix (square, symmetrical, 12×12 elements) is represented in “Eq. 1”:

$$[K_c(\Omega t)] \begin{Bmatrix} X_1 \\ X_2 \end{Bmatrix} = \begin{bmatrix} a & c & p & q & w & m & -a & c & -p & q & -w & -m \\ & e & -q & r & i & 0 & -c & f & q & s & -i & 0 \\ & & b & -d & k & n & -p & -q & -b & -d & -k & -n \\ & & & h & j & 0 & -q & s & d & g & -j & 0 \\ & & & & t & 0 & -w & -i & -k & -j & -t & 0 \\ & & & & & u & -m & 0 & -n & 0 & 0 & -u \\ & & & & & & a & -c & p & -q & w & m \\ & & & & & & & e & q & r & i & 0 \\ & & & & & & & & b & d & k & n \\ & & & & & & & & & h & j & 0 \\ & & & & & & & & & & t & 0 \\ & & & & & & & & & & & u \end{bmatrix} \begin{Bmatrix} x_1 \\ \vartheta_{y1} \\ y_1 \\ \vartheta_{x1} \\ z_1 \\ \vartheta_{z1} \\ x_2 \\ \vartheta_{y2} \\ y_2 \\ \vartheta_{x2} \\ z_2 \\ \vartheta_{z2} \end{Bmatrix} \quad (1)$$

where the coefficients are defined as:

$$a = \frac{12J_y E}{(1+\phi)l_c^3} \quad b = \frac{12J_x E}{(1+\phi)l_c^3} \quad c = \frac{6J_y E}{(1+\phi)l_c^2} \quad d = \frac{6J_x E}{(1+\phi)l_c^2} \quad e = \frac{(4+\phi)J_y E}{(1+\phi)l_c} \quad (2)$$

$$f = \frac{(2-\phi)J_y E}{(1+\phi)l_c} \quad g = \frac{(2-\phi)J_x E}{(1+\phi)l_c} \quad h = \frac{(4+\phi)J_x E}{(1+\phi)l_c} \quad p = -\frac{12J_{xy} E}{(1+\phi)l_c^3} \quad q = -\frac{6J_{xy} E}{(1+\phi)l_c^2} \quad (3)$$

$$r = \frac{(4+\phi)J_{xy} E}{(1+\phi)l_c} \quad s = \frac{(2-\phi)J_{xy} E}{(1+\phi)l_c} \quad t = \frac{EA}{l_a} \quad u = \frac{GJ_p}{l_t} \quad \phi = \frac{12EJ}{GS l_c^2} \quad (4)$$

i, j, k, m, n, w , are cross coupling coefficients which need to be tuned, the parameter ϕ accounts for the shear effects, E and G respectively are the Young's modulus and the shear modulus, S is the cross section area. The different lengths l_c, l_a and l_t responsible for the direct stiffness have also to be tuned by means of the 3D model.

As an example the ratio of “equivalent” length l_c to the diameter as a result from 3D calculation, is represented in Fig. 4 (right) as a function of the ratio of the crack depth to the diameter.

The 3D Model

The 3D non linear model allows obviously to calculate also deflections and strains (by taking into account the breathing behaviour).

Figure 5 shows the mesh which has been used for the cracked test beam, with a relative crack depth 50%. Roughly 11000 elements have been used for the analysis of the cracked cylindrical beam. The mesh has been chosen rather “dense” because not only deformations of the cracked specimen, but also stress intensity factors in correspondence of the crack tip have been calculated numerically and compared with those calculated by means of the classical fracture mechanics approach. This comparison allowed to evaluate the accuracy of the model as regards its capability of representing real crack behaviour in the region close to the crack. The elastic limit was never exceeded in the simulations.

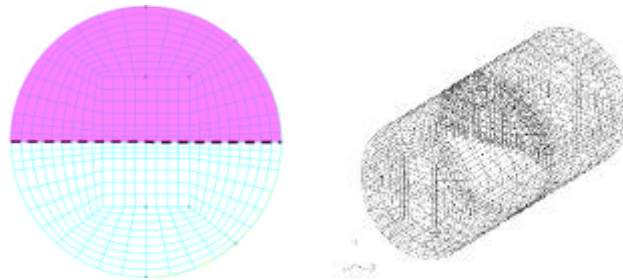


Figure 5. Mesh of the section and isometric view of the model with a crack of 50%. The crack tip is indicated by the dashed line.

Similar meshes have been used for many other crack shapes and crack depths.

The contact model in the cracked surface is obviously non-linear. Also a friction coefficient ($f = 0.2$) has been introduced in order to account for microslip conditions in the cracked area, due to shear forces and torsion. In order to avoid local deformations due to the application of loads, the model has been extended to a higher length where the load is applied to the specimen. This way in the cracked area and in the “measuring” section, where the deflections are evaluated, indicated by the dashed line, no local deformations are present, due to the application of loads. The results obtained with this model will be called simply 3D results.

Recently a new method has been proposed by EDF for deriving from strain energy, calculated by means of a non-linear 3D finite element model, a local crack stiffness which is composed by equivalent springs, connecting the beams which are facing the crack. All these approaches allow to calculate the results in parametric form, so that they can easily be extended to any size of circular section.

COMPARISON OF RESULTS OBTAINED WITH THE 3 MODELS

The 3 different models have been compared by calculating deflections of a test beam in different load conditions. The test beam is a cylinder with a diameter of 25 mm and a length of 50 mm, clamped at one end, and with rotating loads applied to the other end. Figs 6 and 7 show some of the obtained results. In order to highlight the effect of the crack only in all the figures the corresponding displacements of the uncracked beam

have been subtracted. As can be seen the FLEX model seems to be more accurate with respect to the modified SERR model, assuming as reference the 3D calculation. As can be seen especially the effects of tangential stresses due to torsion or shear forces cannot be correctly represented by the modified SERR model.

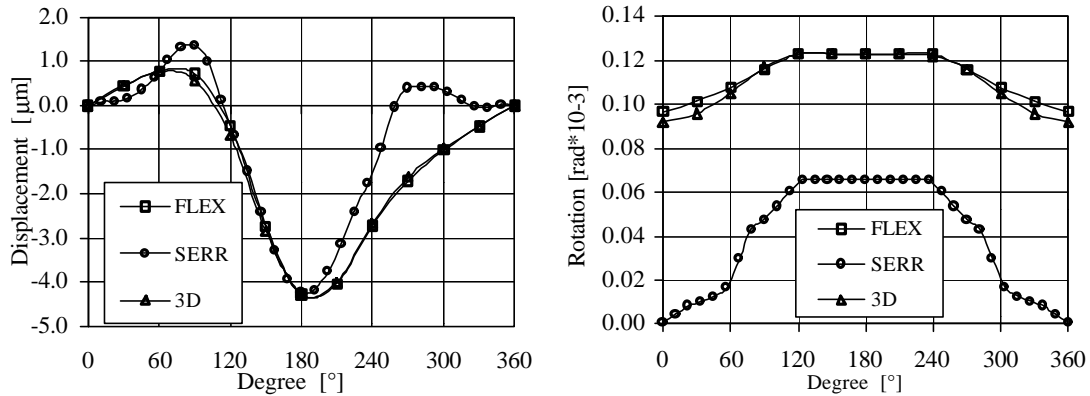


Figure 6. Bending and torsion, 50% crack depth, x displac. (left), ϑ_z rotation (right)

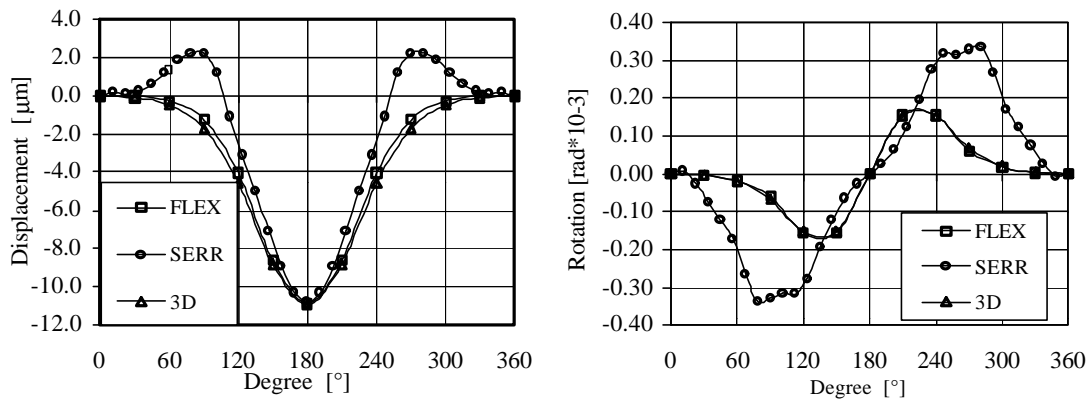


Figure 7. Bending and shear, 50% crack depth, x displacement (left), ϑ_x rotation (right)

THE DYNAMIC BEHAVIOUR OF THE CRACKED ROTATING SHAFT

The model of a cracked shaft line is represented by the traditional 2.nd order matrix differential equation, in which the mass and damping matrices are constant, whilst the stiffness matrix has a variable part, which is function of the breathing behaviour, which in turn is determined by the angular position of the crack with respect to the static and dynamic loads.

When the breathing is mainly due to static loads (such as the weight of horizontal rotors) then the equation is linear and the stiffness is only depending on the angular position of the shaft with respect to the load. Steady state solutions can be found in the

frequency domain by means of an iterative procedure combined with a harmonic balance approach as will be shown here below. Unstable solutions can be found by integrating the equations in the time domain.

When the breathing is mainly influenced by the dynamic loads, which means also by the vibration itself which is generated by the crack, the equation becomes non linear; again the harmonic balance and an iterative procedure can be used in the frequency domain when looking for the steady state solution as it has been done in [4]. For each rotating speed the breathing behaviour can be found iteratively, but the convergence of the solution is not certain.

Also time domain integration can be used. In this case the solution can be a superposition of parametric instability and steady state forced motion. The steady state solution in the frequency domain can be calculated in following way.

When the equivalent beam is introduced in the finite element model of the rotor then the complete stiffness $K_c(\Omega t)$ of the rotor can be calculated and introduced in the differential equation (5):

$$[M]\{\ddot{x}\} + ([R] + [Gyr])\{\dot{x}\} + [K_c(\Omega t)]\{x\} = \{f_e\} + \{w\} \quad (5)$$

The Fourier expansion of the periodic stiffness is truncated in correspondence of the fifth harmonic component.

$$[K_c(\Omega t)] = [K_m] + \sum_{n=1}^5 \frac{1}{2} [K_n] e^{in\Omega t} + \frac{1}{2} [K_n^*] e^{-in\Omega t} \quad (6)$$

Introducing this stiffness in the equations of motion of the rotor:

$$[M]\ddot{x} + ([R] + [Gyr])\dot{x} + [K_m]x = - \left(\sum_{n=1}^5 \frac{1}{2} [K_n] e^{in\Omega t} + \frac{1}{2} [K_n^*] e^{-in\Omega t} \right) \{x\} + \{f_e\} + \{w\} \quad (7)$$

with $\{x\}$ expanded in a Fourier series truncated in correspondence of the fifth harmonic component:

$$\{x\} = \sum_{n=0}^5 \frac{1}{2} \{x_n\} e^{in\Omega t} + \frac{1}{2} \{x_n^*\} e^{-in\Omega t} \quad (8)$$

The equivalent force component vectors are then obtained by:

$$\left(\frac{1}{2} \sum_{n=1}^5 [K_n] e^{in\Omega t} + [K_n^*] e^{-in\Omega t} \right) \{x\} = \frac{1}{2} \sum_{n=0}^5 \{f_n\} e^{in\Omega t} + \{f_n^*\} e^{-in\Omega t} \quad (9)$$

where f_n depend on x and have therefore to be calculated with an iterative procedure, until convergency is reached. The static and dynamic behaviour of a cracked rotor can be calculated for each rotating speed using above equation.

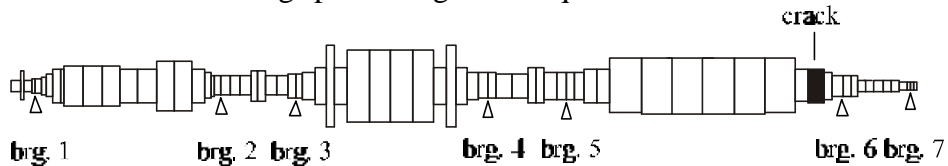


Figure 8. Model of a 320 MW turbogroup.

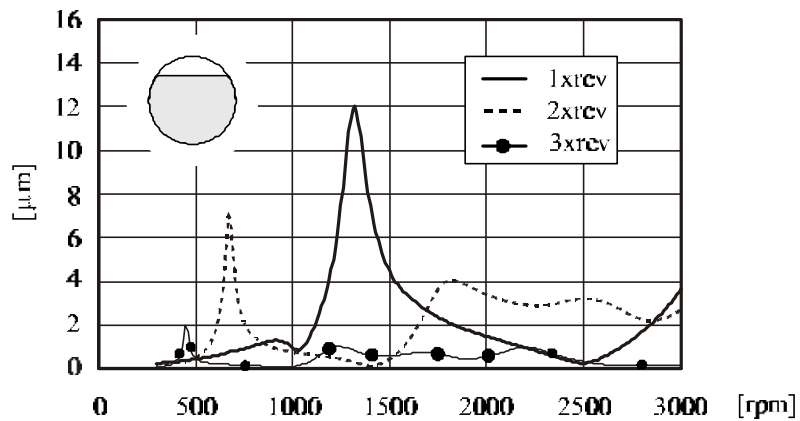


Figure 9. Vertical vibration amplitude vs. speed in bearing 6: 30% crack depth.

Figure 9 shows the results obtained with described procedure on the turbogroup of Fig. 8, as an example. The sensitivity of the dynamic behaviour of turbogroups to the position and depth of the crack has been studied in [5] and [6].

CONCLUSIONS

The models used to represent the behaviour of cracked shafts have been described and compared. Some results obtained with a simplified 1D model have shown to be rather accurate, and have been used to calculate the dynamic behavior of cracked rotor systems by means of an harmonic balance approach and an iterative procedure, which proved to be accurate and reliable.

REFERENCES

1. Gasch, R. (1993) A survey of the dynamic behaviour of a simple rotating shaft with a transverse crack. *Journal of Sound and Vibration* **160** (2), 131-332.
2. Dimarogonas, A.D. (1996). Vibration of cracked structures. A state of the art review. *Engineering Fracture Mechanics* **55**, 831-857
3. Wauer, J. (1990) On the dynamics of cracked rotors: a literature survey. *Applied Mechanics Reviews* 43, No.1, 13-17.
4. Bachschmid, B. and Tanzi, E. (2002) Non-Linear effects in cracked rotors. *IFTOMM, Proceedings of Sixth International Conference on Rotor Dynamics*, Sydney, Oct. 2002 pp. 358-365.
5. Bachschmid, N., Pennacchi, P., Tanzi, E. and Audebert, S. (2001) Dynamical Behaviour of cracked rotors: a sensitivity analysis. *Methodes de surveillance et techniques de diagnostic acoustiques et vibratoires*, Compiègne (France), 16-18 october 2001, pp. 517-529.
6. Bachschmid, N. and Tanzi, E. (2002) Vibration Pattern Related to Transverse Cracks in Rotors. *Shock and Vibration* **9**, No. 4-5, ISSN 1070-9622, 217-224.